Nigerian Journal of Physics (NJP)

ISSN: 1595-0611

Volume 32(3), September 2023

Influence of Doping Concentration on Photocatalytic Activity of Bismuth-Doped Titanium (IV) Oxide

[1]Olaniyi, K. J., [1]Ogundeji, A. O., [1]Adewale, T. N., [2]Adegboyega, O., [1,3]Awodele, M. K., *[1,3]Adedokun, O.

[1]Department of Pure and Applied Physics, Ladoke Akintola University of Technology, Ogbomoso, Nigeria.
[2]Department of Physical Science Education, Emmanuel Alayande University of Education, Oyo, Nigeria.
[3]Nanotechnology Research Group (NANO+), Ladoke Akintola University of Technology, Ogbomoso, Nigeria.

*Corresponding author's email: oadedokun@lautech.edu.ng Phone: +2347031195750

ABSTRACT

Titanium (IV) Oxides (TiO_2) have been widely studied for photocatalytic applications due to their excellent electrical and optical properties. It has a band gap of 3.0 – 3.2eV and can be excited by ultraviolet (UV) light. Although TiO_2 has been researched to be an efficient photocatalyst material by many researchers, its wide band gap limits its absorption of light into the UV portion of the electromagnetic spectrum. In this work, we reported a straightforward Sol-gel approach to synthesize both undoped and Bismuth (Bi) doped TiO_2 in order to investigate the photocatalytic activity of Bi-TiO_2. Various characterization methods, including XRD, FTIR, and DRS, were employed to investigate how the doping concentration of Bi affected the optical and structural characteristics of TiO_2. From the results, the XRD spectrum indicated the tetragonal structure corresponding to the anatase phase of TiO_2. DRS reveals that there is a slight decrease in the energy band gap for the sample from 3.23 eV – 3.15 eV as the concentration of Bi increases. The degradation of methylene blue and methylene orange through photocatalysis was used to examine the samples' photocatalytic activity. The outcomes of the photocatalytic activity showed that the undoped TiO_2 has a better photocatalytic degradation percentage of 89.27% and 58.19% for Methylene blue and Methylene orange, respectively when compared with the Bi-TiO_2 samples.

Keywords:
TiO_2,
Bi doped TiO_2,
Sol-gel,
Photocatalytic activity.

INTRODUCTION

Water pollution is one of the major environmental challenges due to the growing demand for clean water for human use in the modern world. Even in small amounts, some dyes found in wastewater are regarded as pollutants and are typically harmful to people and other living things. The main causes of environmental and water pollution are industrial wastes from the paper and textile industries, household wastewater, and other sources. These pollutants seriously endanger aquatic and environmental life (Li et al., 2020; Rafiq et al., 2021; Shittu et al., 2023).

In recent times, various strategies have been proposed and employed to remove pollutants in wastewater. Some of these methods include flocculation, coagulation, precipitation, adsorption, ion exchange, etc (Toxicol et al., 2016). Most of these methods are not suitable for large-scale applications due to their high cost. Also, the majority of these techniques don't totally break down the hazardous substances., they only generate a less toxic product. However, there has been a lot of research in this area in the last few years, and significant advancements have been noted. In particular, photocatalysis is now thought to be a viable substitute for effectively eliminating dyes from wastewater. One type of Advanced Oxidation Technology (AOT) is photocatalysis, which is based on physicochemical processes that alter the chemical structures of organic compounds and cause them to mineralize (Pant et al., 2019). In recent years, the photo-degradation of pollutants has become increasingly popular. The process of photocatalysis involves heterogeneous catalysis, in which light is absorbed by a semiconductor photocatalyst to break down a variety of environmental pollutants, such as organic pollutants found in the wastewater. When compared to conventional wastewater treatment techniques, photodegradation offers benefits. For instance, at room temperature, active photocatalysts can completely degrade organic pollutants in a matter of hours. Furthermore, organic pollutants can fully mineralize into relatively nonhazardous products (water and CO_2) without

producing secondary toxic products (Shivaraju et al., 2017).

Metal oxide semiconductors, such as Stanic Oxide (SnO_2), Titanium (IV) oxide (TiO_2), and Zinc oxide (ZnO) are highly desirable and auspicious materials for both fundamental research and real-world applications because of their chemical inertness, high activity, non-toxicity, and affordability (Bhatti et al., 2021; Him et al., 2019; Saravanan & Soga, 2021; Shittu et al., 2023). Since ancient times, paint additives containing titanium dioxide (TiO_2) have been widely used to create white pigments. One of the most often used metal oxides is titanium (IV) oxide (TiO_2), which has strong photocatalytic activity and doesn't produce any secondary pollutants. (Him et al., 2019). It is well-known for a number of characteristics, including high photoactivity, excellent stability, affordability, and non-toxicity. TiO_2-based nanostructures have been extensively researched in academic studies over the past few decades and have been applied to a wide range of applications, including energy storage, photovoltaics, sensors, and the elimination of organic pollutants and pathogens (Pant et al., 2019).

Three crystalline forms of TiO_2 are known to exist: rutile, anatase, and brookite. While rutile and anatase are the ideal phases for photocatalysis, brookite is thought to be the least stable phase and is not typically utilized for this purpose (Haider et al., 2019). Both rutile and pure anatase structure have band gaps of 3.0 eV and 3.2 eV, respectively. As a result, only the near ultraviolet (UV) spectrum of solar radiation can be absorbed by pure TiO_2. The recombination time of free radicals must be extended or the phase composition must be altered to significantly alter the material's optical and electrical properties in order to modify this property and shift the excitation threshold toward higher wavenumbers. This can be accomplished by doping TiO_2 with different metal or non-metal substances (Nazlı, 2020).

Also, the process employed in the synthesis of a photocatalyst has a significant impact on its characteristics and photocatalytic activity. Various methods have been employed to synthesize different photocatalyst materials such as sol-gel (Gorgani & Koozegar, 2020; Pant et al., 2019; Razani et al., 2017; Shivaraju et al., 2017; Solís-Casados et al., 2018), hydrothermal (Cheng et al., 2018), sonochemical (Boini et al., 2018), co-precipitation (Kareem et al., 2022; Shukla et al., 2022), etc.

Photocatalytic activity of TiO_2 has been reported by many researchers to be enhanced by doping with various metals using different methods of synthesis. Shivaraju *et al*., prepared Magnesium doped TiO_2 [Mg-TiO_2] using a mild sol-gel technique and was characterized by XRD, SEM, and FTIR. From the characterization of the sample, it was observed that the sample shows mixed anatase and rutile phases with excellent crystallinity, structural elucidation and consequently shifting of the energy band gap. The synthesized and characterized Mg-TiO_2 was reported to show excellent photocatalytic degradation efficiency. In another work by Toxicol *et al.,* Magnesium doped titanium dioxide (Mg^{+2}-TiO_2) was synthesized using the sol-gel method and characterized using XRD, UV-Visible, XPS, SEM, and FT-IR techniques. The magnesium weight percentages ranged from 0.25 to 1.0 wt.%. The outcome showed that Mg^{+2} had no effect on the TiO_2 crystal patterns. Methyl orange dye (MO) photocatalytic degradation was used to test the photocatalytic efficiency of the synthesized catalysts under visible light irradiation. The results showed that the Mg^{+2}-TiO_2 catalysts had higher catalytic activity than the undoped TiO_2 catalysts. Yilleng *et al.,* prepared 1% Ag-TiO_2, 3% Ag-TiO_2, and 5% Ag-TiO_2 and applied it to degrade Chlorazole black E and it was found that doping TiO_2 with Ag at higher concentration does not enhance the activity of TiO_2. Saravanan and Soga conducted a study wherein they synthesized pure and Ag-doped TiO_2 nanoparticles for the purpose of photocatalytically degrading methylene blue. Using UV-visible spectroscopy and x-ray diffraction (XRD), the synthesized materials were examined. The various structural phases and crystallite sizes of the nanoparticles were displayed by the XRD results. The subsequent addition of Ag dopant resulted in a decrease in the photocatalysts' band gap. Methylene blue (MB) was photocatalytically degraded for up to 90 minutes in the presence of sunlight for both pure and Ag-doped TiO_2 nanoparticles. It was determined that the duration of irradiation directly correlated with the enhancement of photocatalytic degradation of MB dye caused by the addition of Ag as a dopant into TiO_2 crystal. Moreover, Sol-gel Synthesis of Fe_2O_3-doped TiO_2 for Enhanced Photocatalytic Degradation of 2,4-Dichlorophenoxyacetic Acid was conducted in a study by Razani et al. It was discovered that the tetragonal, crystalline anatase TiO_2 cell structure dominated the catalysts that were generated. The 0.05wt% Fe_2O_3 doped TiO_2 catalyst demonstrated higher photocatalytic activity than undoped TiO_2, according to the results of the photocatalytic degradation experiment. However, as the Fe_2O_3 content increased, the catalyst's performance decreased because of a potential increase in recombination centers. In this work, we investigated the photocatalytic activity of Bi-TiO_2 at concentration of 1%, 2%, 3% and 4% applying it to a modeled methylene blue and methylene orange dye. The preparation of TiO_2 and Bi-TiO_2 at concentrations 1%, 2%, 3% and 4% was done by Sol-gel method and characterized using X-ray Diffraction (XRD), Fourier Transform Infra-Red (FTIR) spectroscopy and Diffuse Reflectance Scattering (DRS).

MATERIALS AND METHODS

Preparation of pure TiO_2

Undoped TiO_2 nanoparticles are synthesized by sol-gel technique using Titanium isopropoxide $C_{12}H_{28}O_4Ti$ (TTIP) as a starting material. In the synthesis, 13 ml of 2-Propanol was dropped into a beaker and 10 ml of acetic acid was added slowly. The solution was stirred for few minutes. After which 5 ml TTIP was added to the solution and it was stirred vigorously under magnetic stirrer for 15 minutes. 61 ml of de-ionised water was added drop wisely within 10 minutes to the solution and stirred continuously for 4hours. Consequently, the obtained solution was aged for 24 hours at a room temperature. As prepared TiO_2 gel were dried at 100ºC for few hours (at least 5 hours). Finally, the obtained powder samples were ground and finally annealed at 500ºC for 3 hours.

Preparation of Bi-doped TiO_2

In a typical synthesis of bismuth doped TiO_2, bismuth nitrate was dissolved in 61ml of deionized water at room temperature, stirred for 30 minutes to obtain a solution X. Solution Y was obtained by dissolving 5 ml of TTIP into 13 ml of 2-propanol and 10 ml of acetic acid, was stirred for 30 minutes. Then solution X was dropped wisely into the solution within 10 minutes under continuous vigorous stirring. The obtained solution was stirred for 2 hours at room temperature and left to age for 24 hours. The synthesized doped TiO_2 gel were dried for few hours at 100ºC. The powder was pulverized and annealed at 500ºC for 3 hours.

Characterization Technique

A powdered X-ray technique was employed by Rigaku X-ray diffractometer with monochromatic Cu Kβ with wavelength (λ= 1.5406Å) at 40 kV and 30 mA to study the samples' grain size and crystallography. Within the scanning range of 10° to 80°, all samples had a scanning speed of 2.0156°. An FTIR spectrometer made by PerkinElmer was used to examine the samples' structural composition. Equation 1 gives the Kubelka-Munk's equation and the relation was used to determine the energy bandgap using the diffuse reflectance spectroscopy (DRS) technique (Kareem et al., 2022; Shukla et al., 2022).

$$F(R_\infty) = \frac{(1-R_\infty)^2}{2R_\infty} \qquad (1)$$

F(R) is proportional to the extinction coefficient (α), where R is the reflectance.

Photocatalytic experiment

Under direct sunlight, the synthesized samples photocatalytic activity was tested to break down a modeled methylene blue (MB) and methyl orange (MO) dye. Throughout the experiment, all other parameters remained the same, with the exception of the intensity of the sun. Distilled water was used to prepare the dye solution, which had a neutral pH and concentration of 2.5 mol/L. A volumetric flask containing 1000 ml of 10 ppm MB solution was prepared. The reaction vessel, a 250 ml beaker, was set up on a magnetic stirrer. After adding 15 mg of photocatalyst for every 25 ml of dye solution, stirring for 20 minutes resulted in the formation of a suspension. After the suspension reached an equilibrium between adsorption and desorption in the dark for thirty minutes, it was exposed to solar irradiation for two hours. Three milliliters of the samples were taken and centrifuged for five minutes for separation at the designated time intervals (0 min, 20 min, 40 min, and 60 min). A UV-visible spectrophotometer was used to measure the absorbance of the supernatant, and equation 2 was used to compute the percentages of degradation (Kareem et al., 2022; Shittu et al., 2023):

$$D = \frac{C_i - C_f}{C_i} \times 100\% \qquad (2)$$

here Ci stands for the initial concentration of the dyes and C_f for their final concentration. Concurrently, the dye solution was subjected to solar radiation in the absence of a catalyst for the control experiment. The following acronyms are used in relation to the photocatalytic activity:

BT-4: Methyl Blue + Pure TiO_2
BBT-1: Methyl Blue + Bismuth doped TiO_2 at 1%
BBT-2: Methyl Blue + Bismuth doped TiO_2 at 2%
BBT-3: Methyl Blue + Bismuth doped TiO_2 at 3%
BBT-4: Methyl Blue + Bismuth doped TiO_2 at 4%
OT-4: Methyl Orange + Pure TiO_2
OBT-1: Methyl Orange + Bismuth doped TiO_2 at 1%
OBT-2: Methyl Orange + Bismuth doped TiO_2 at 2%
OBT-3: Methyl Orange + Bismuth doped TiO_2 at 3%
OBT-4: Methyl Orange + Bismuth doped TiO_2 at 4%

RESULTS AND DISCUSSION

X-ray Diffraction Study

The X-ray diffraction patterns of the undoped and Bismuth doped titanium (IV) oxide nanoparticles prepared by sol-gel method is shown in the figure 1a. The graph reveals the intensity peaks at concentration of 0%, 1%, 2%, 3% and 4%. Figure 1b show the morphological property of Titanium (IV) oxide in terms of crystalline size and the full width at half maximum (FWHM). The crystalline size of peak of the plots was calculated using Scherrer's equation using the most pronounced peaks of the undoped and doped TiO_2. Figure 1b show the variation between the crystalline sizes (D) and full width at half maximum with respect to concentration. As the crystalline size decreases, Full Width at Half Maximum (degrees) increases with increase in the concentration of dopant (percentage). The peaks corresponding to 2θ= 25.50688, 25.46163, 25.44482, 25.49128 and 25.42403 shows that TiO_2

consists of majorly anatase phase with crystalline nature (Solís-Casados et al., 2018). The strongest peak (110) is gradually moved towards a lower 2theta degree by the addition of Bi nanoparticles. But as can be seen from the XRD pattern shown in figure 1c, the peak at 3% Bi-TiO_2 nanoparticles continued to be in line with the peak of pure TiO_2. This indicates that the loading of Bi into the TiO_2 lattice is successful. Equation 3 illustrates the application of Scherrer's equation to determine the samples' crystallite sizes. (Kareem et al., 2022; Shittu et al., 2023; Xie et al., 2018). Table 1 shows the crystalline size, FWHM, glancing angle and intensity for undoped and bismuth doped TiO_2 at various concentrations. The Scherrer's equation is given by:

$$D = \frac{k\lambda}{\beta cos\theta} \quad (3)$$

where β is the full width at half maxima (FWHM), θ is the glancing angle, λ is the experimental wavelength, or 1.5406Å, and 0.98 is the shape factor. D is the crystallite size in nanometers.

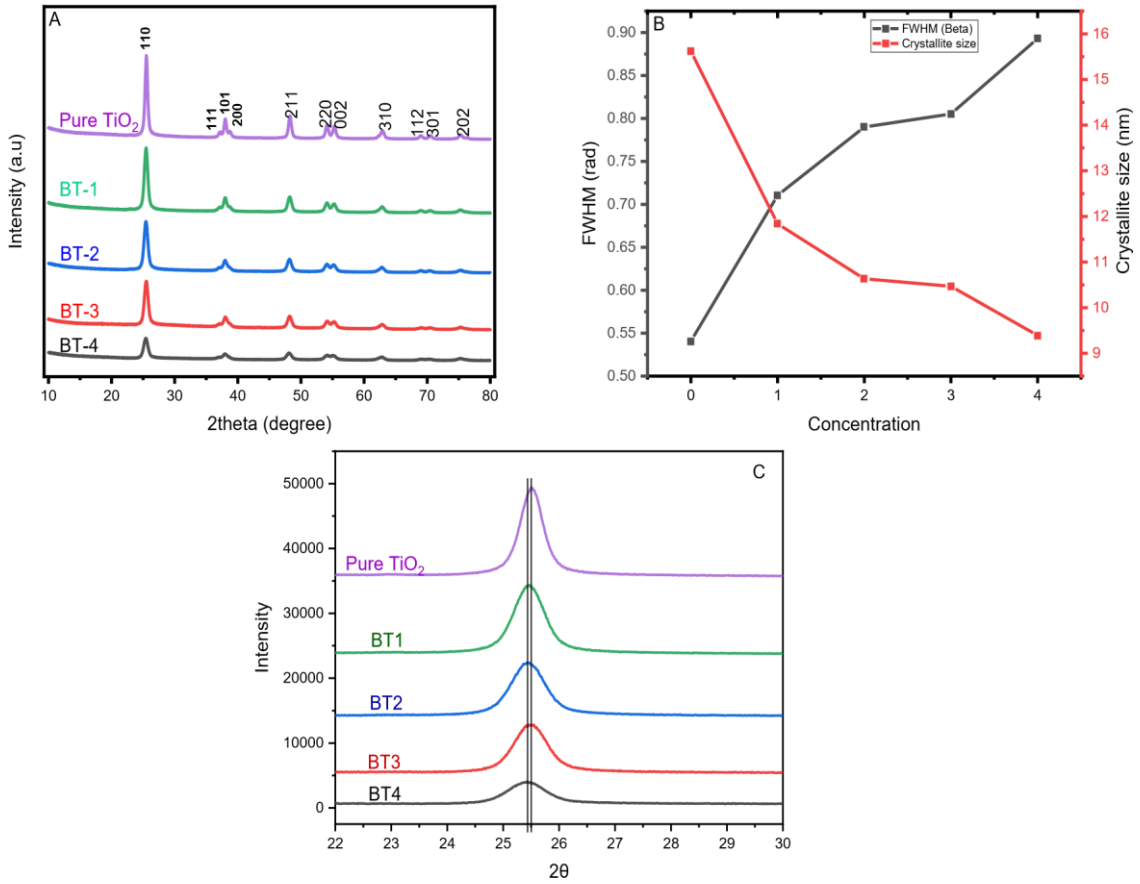

Figure 1: (a) X-ray diffraction peaks (b) A graph showing the relationship between crystalline size, Full Width at Half Maximum and concentration at peaks.

Table 1: The crystalline size, FWHM, glancing angle and intensity for undoped and Bi-TiO_2 at concentrations 1 – 4%.

Concentration (%)	Crystallite size in (D) (nm)	FWHM (degree)	2θ (degree)	Intensity (a.u)
0	15.62011	0.54063	25.50688	14231.5202
1	11.83758	0.71052	25.46163	26825.6625
2	10.63204	0.79001	25.44482	36920.5021
3	10.47061	0.80535	25.49128	46566.2483
4	9.39005	0.89309	25.42403	51838.2148

Fourier Transform Infrared Spectroscopy

FTIR analysis was used to determine the functional group of the synthesized samples. The obtained spectra from the FTIR analysis for synthesized TiO_2 and Bi-TiO_2 were shown in Figure 2. The peak at 3411.09881 cm^{-1} in the infrared spectra of the undoped TiO_2

nanoparticles was attributed to the O-H stretching vibration, indicating the presence of a hydroxyl group., the peak 490.592886 cm^{-1} show the stretching vibration of Ti-O, the peak 1627.50988 cm^{-1} show the stretching vibration of Ti-O-Ti while the peak at 3684.44269 cm^{-1} indicate the presence of amines; while the presence of alkynes, aromatic rings, pyridines, and thiophenes are shown in the spectra of BT1 to BT-4.

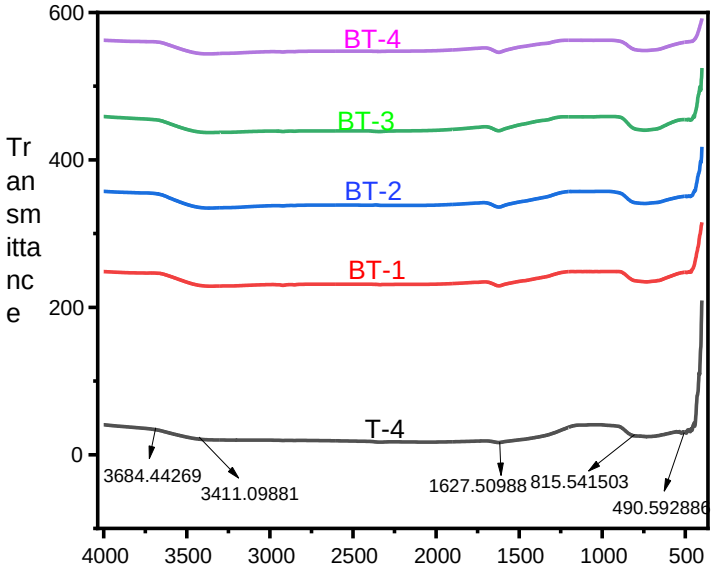

Figure 2: A graph of Transmittance against wave number

Diffuse Reflectance Spectroscopy

Diffuse reflectance scattering (DRS) technique was used to examine the optical properties of both undoped and Bi-doped TiO_2 within the 200-900 nm scanning range. Figure 3a shows the absorption spectra of pure TiO_2 and Bi-TiO_2. The absorbance for the samples increases with increasing wavelength from around 200nm to 320nm, it shows a decrease trend from 320nm to 600nm with increase in wavelength except for pure TiO_2 which is from 320 – 430nm and then a linear trend henceforth. It can also be deduced from figure 3a that Bismuth doped TiO_2 at 3% has the highest absorbance peak followed by 2%, 4% and then 1%. Also, the reflectance spectra are shown in figure 3b.

The samples' energy band gap was ascertained using the Kubelka-Munk relation. Table 2 displays the estimated band gap for each sample, and Figure 3c shows this information graphically. As Table 2 illustrates, the obtained results show that the band gap in TiO_2 narrows from 3.23 eV to as low as 3.15 eV as the concentration of Bi increases; these low band gap values make this material potentially active under light illumination in the visible region of the electromagnetic spectrum (Solís-Casados et al., 2018).

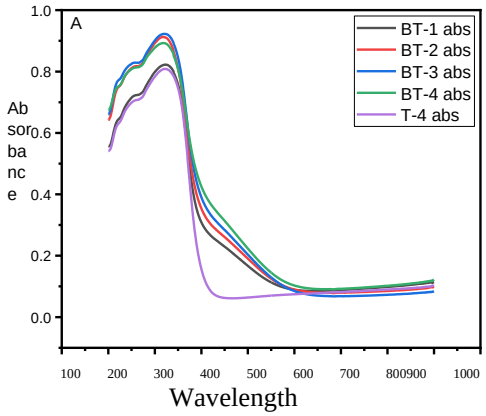

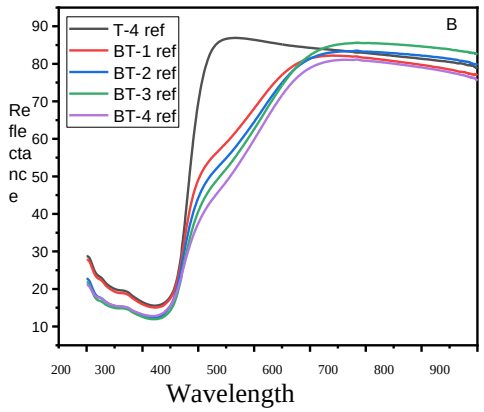

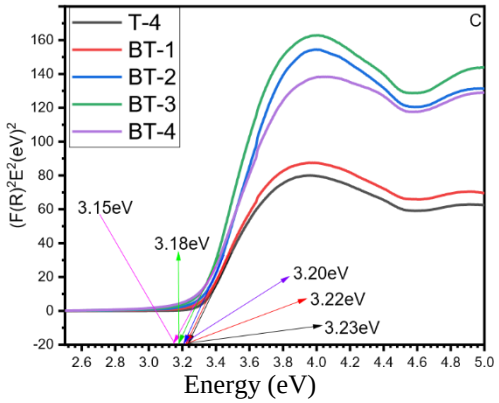

Figure 3: (a) DRS absorbance spectra for undoped and Bi doped TiO_2 (b) DRS reflectance spectra for undoped and Bi doped TiO_2 (c) Tuac plot showing energy band gaps of undoped and Bi doped TiO_2

Table 2: Energy band gap and absorption maximum for doped and undoped TiO_2

Sample	Energy (eV)	Absorption peak (nm)
T-4 (Pure TiO_2)	3.23	322
BT-1	3.22	323
BT-2	3.20	319
BT-3	3.18	320
BT-4	3.15	319

Photocatalytic Activity

The degradation of the MB and MO dyes under solar light irradiation was employed to measure the photocatalytic activities of TiO_2 and Bi-TiO_2. The absorption spectra of an aqueous solution of 50 ml MB and MO with 30 mg of the various photocatalysts under solar light irradiation for varied time intervals are displayed in Figures 4 (a-e) and 5 (a-e). As the exposure time increases, it can be seen that the absorption peaks rapidly decrease, indicating the degradation of MB dye. The absorbance spectrum of UV-Vis was measured between 200 and 900 nm, with absorbance maxima noted at 664 nm and 466 nm for methyl blue and methyl orange respectively. The absorption peak of the samples continuously decreases with increase in exposure time (60 min). Though as expected that the percentage degradation of TiO_2 should increase as the band gap of the samples is tuned toward the visible region with increase in the concentration of bismuth dopant, reverse is the case, as the concentration of dopant increase from 1% to 4%, percentage degradation decreases. The TiO_2 photocatalyst's metal load is the cause of this behaviour. Because active molecules are deactivated by collisions with ground state molecules, which dominate the reaction, the photocatalytic activity of TiO_2 photocatalyst decreases with increasing metal load. (Yilleng *et al.*, 2019). Figure 6 and 7 shows the rate of concentration degradation and percentage degradation of MB and MO dye against time respectively. The percentage degradation of each sample was calculated using equation 3 (Kareem et al., 2022; Shittu et al., 2023). The calculated percentage degradation for each of the sample is shown in table 3.

$$D = \frac{C_i - C_f}{C_i} \times 100\% \quad (3)$$

where Ci stands for the initial concentration of the dyes and C_f for their final concentration.

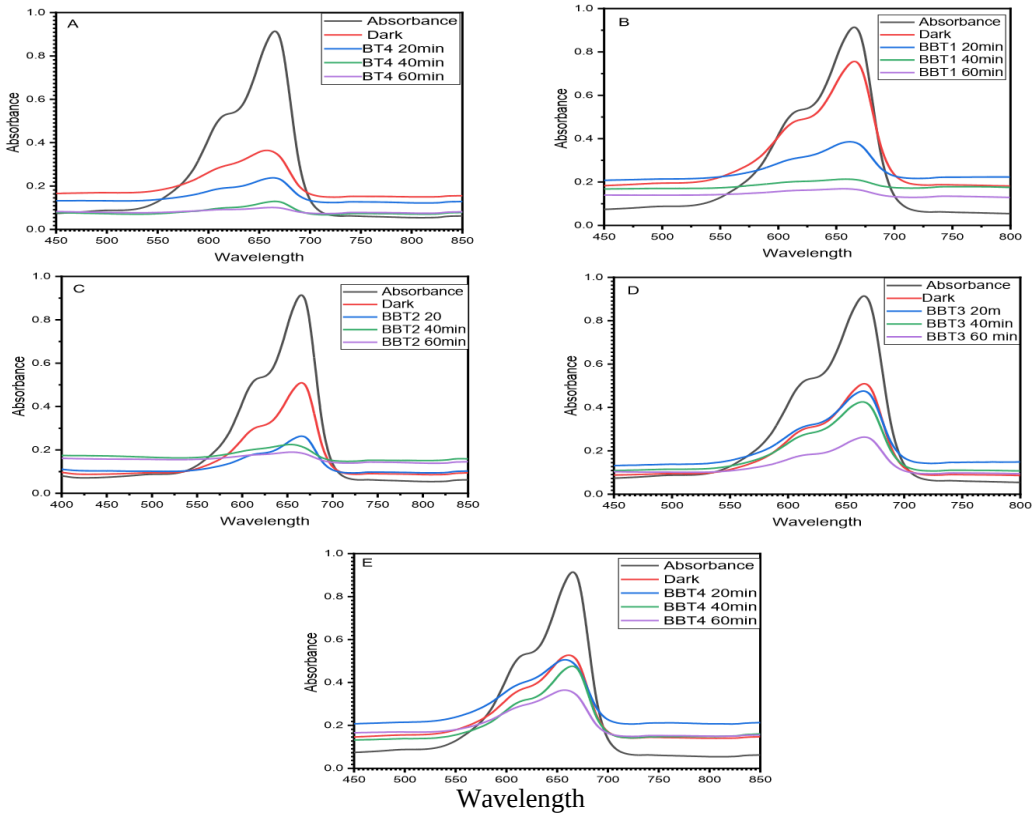

Figure 4: Absorbance spectra of pure TiO_2, 1%, 2%, 3%, and 4% Bi-TiO_2 nanoparticles in MB solution under solar irradiation.

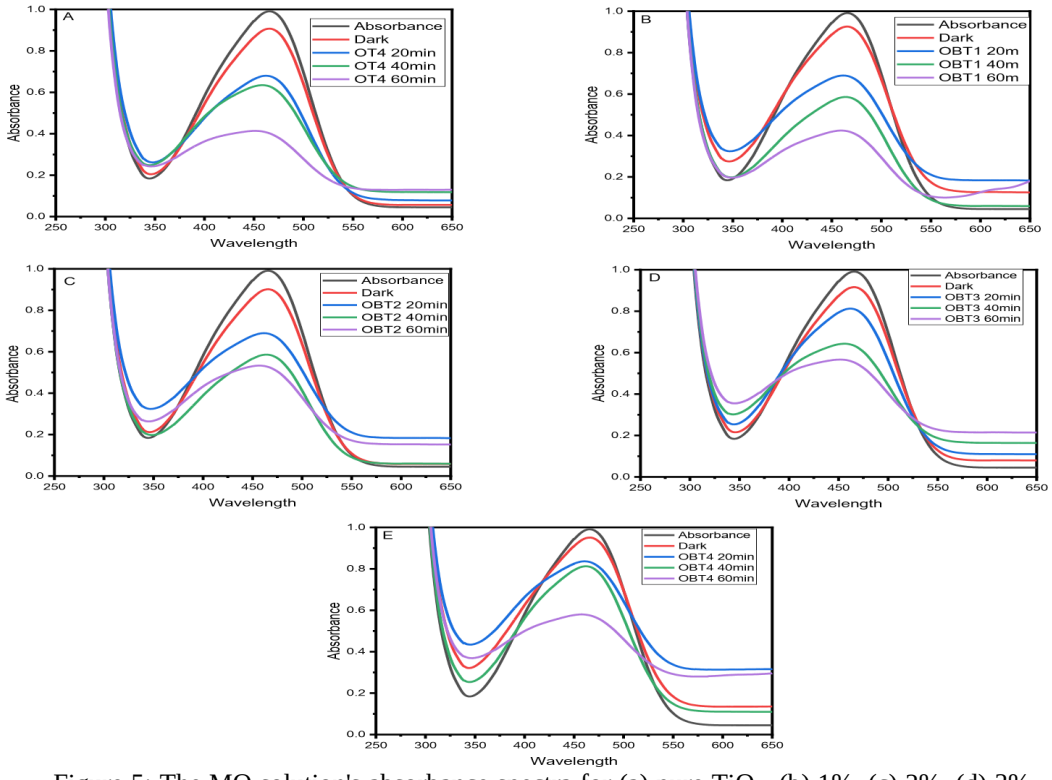

Figure 5: The MO solution's absorbance spectra for (a) pure TiO_2, (b) 1%, (c) 2%, (d) 3%, and (e) 4% Bi-TiO_2 nanoparticle under solar irradiation.

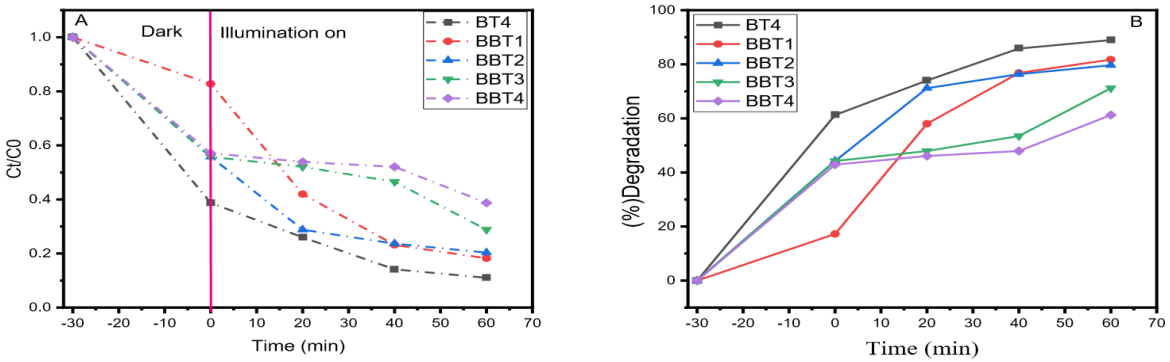

Figure 6: (a) Rate of MB dye concentration degradation over time (b) Percentage Degradation against time plot for each sample in MB

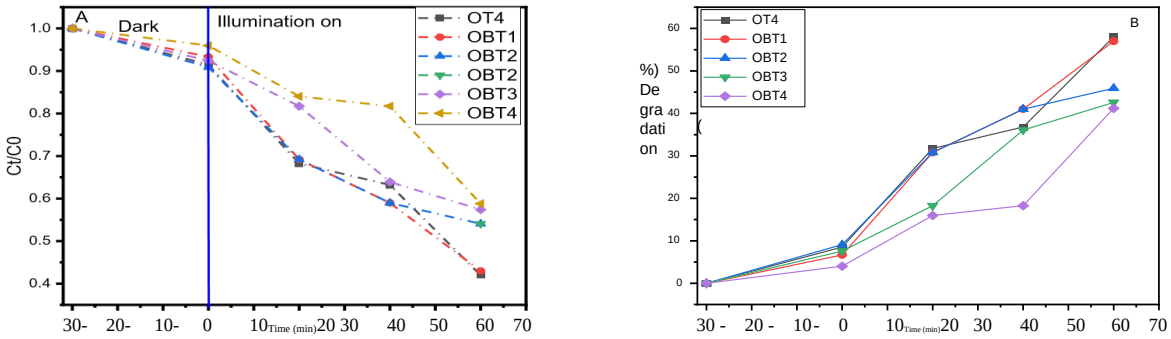

Figure 7: (a) Rate of MO dye concentration degradation over time (b) Percentage Degradation against time plot for each sample in MO

Table 3: Percentage degradation of Samples

Sample	C_t	C_0	$C_0 - C_t$	$(C_0 - C_t)/C_0$	%Degradation
BT4	0.098	0.913	0.815	0.89266	89.26616
BBT1	0.17	0.913	0.743	0.8138	81.38007
BBT2	0.186	0.913	0.727	0.79628	79.6276
BBT3	0.262	0.913	0.651	0.71303	71.3034
BBT4	0.36	0.913	0.553	0.6057	60.56955
OT4	0.416	0.995	0.579	0.58191	58.19095
OBT1	0.426	0.995	0.569	0.57186	57.18593
OBT2	0.536	0.995	0.459	0.46131	46.13065
OBT3	0.569	0.995	0.426	0.42814	42.81407
OBT4	0.583	0.995	0.412	0.41407	41.40704

CONCLUSION

In this study, undoped TiO_2 and Bi-TiO_2 at concentration 1-4% were successfully synthesized by Sol-gel method. X-ray diffraction analysis reveals that the crystallite size of the undoped TiO_2 is 15.62011 nm. This Crystalline size decreases with increase in concentration of Bismuth as dopant. FTIR was used to determine the various functional groups in TiO_2 nanoparticles. Diffuse Reflectance Spectroscopy was used to determine the effect of doping on the optical properties of the samples. It was found that undoped TiO_2 and Bi-TiO_2 (from 1% to 4%) has the band gap of 3.23eV, 3.22eV, 3.20eV, 3.18eV and 3.15eV, respectively. The degradation model of a methylene blue and methylene orange dyes was used to assess the samples' photocatalytic activity. From the results of percentage degradation evaluated, it can be concluded that doping TiO_2 with Bismuth at 1%, 2%, 3%, and 4% does not improve the photo degradation performance of TiO_2 but rather reduces it.

ACKNOWLEDGEMENTS

OA gratefully acknowledges the Department of Science & Technology (Govt. of India) for the award of 2019/2020 Research Training Fellowship for Developing Countries Scientist (RTF-DCS). The authors acknowledge with gratefulness the Centre for

High-Pressure Research, Bharathidasan University, India for sample characterizations.

REFERENCES

Bhatti, M. A., Shah, A. A., Almaani, K. F., Tahira, A., Chandio, A. D., Willander, M., Nur, O., Mugheri, A. Q., Bhatti, A. L., Waryani, B., Nafady, A., & Ibupoto, Z. H. (2021). *TiO_2 / ZnO Nanocomposite Material for Efficient Degradation of Methylene Blue*. *21*(4), 2511–2519. https://doi.org/10.1166/jnn.2021.19107

Boini, S., Reddy, N., Ruchira, N., & Aneesha, S. (2018). *Structural and Morphological Studies of TiO_2 Nanorods Synthesized by Sonochemical Route Structural and Morphological Studies of TiO_2 Nanorods synthesized by sonochemical route*. *September 2019*. https://doi.org/10.30967/ijcrset.1.1.2018.49-51

Cheng, H. H., Chen, S. S., Yang, S. Y., Liu, H. M., & Lin, K. S. (2018). Sol-Gel hydrothermal synthesis and visible light photocatalytic degradation performance of Fe/N codoped TiO_2 catalysts. *Materials*, *11*(6). https://doi.org/10.3390/ma11060939

Gorgani, M., & Koozegar, B. (2020). Structural , photocatalytic and surface analysis of Nb / Ag codoped TiO_2 mesoporous nanoparticles. *Journal of Sol-Gel Science and Technology*, 728–741. https://doi.org/10.1007/s10971-020-05403-y

Haider, A. J., Jameel, Z. N., & Al-Hussaini, I. H. M. (2019). Review on: Titanium dioxide applications. *Energy Procedia*, *157*, 17–29. https://doi.org/10.1016/j.egypro.2018.11.159

Him, C., Tsang, A., Li, K., Zeng, Y., Zhao, W., Zhang, T., Zhan, Y., & Xie, R. (2019). Titanium oxide based photocatalytic materials development and their role of in the air pollutants degradation : Overview and forecast. *Environment International*, *125*(December 2018), 200–228. https://doi.org/10.1016/j.envint.2019.01.015

Kareem, M. A., Bello, I. T., Shittu, H. A., Sivaprakash, P., Adedokun, O., & Arumugam, S. (2022). Synthesis , characterization , and photocatalytic application of silver doped zinc oxide nanoparticles. *Cleaner Materials*, *3*(January), 100041. https://doi.org/10.1016/j.clema.2022.100041

Li, R., Li, T., & Zhou, Q. (2020). *Impact of Titanium Dioxide (TiO 2) Modification on Its Application to Pollution Treatment — A Review*.

Nazlı, D. (2020). *Preparation of Doped TiO 2 photocatalysts and their decolorization*. *8*(3), 655–663. https://doi.org/10.21923/jesd.672207

Pant, B., Park, M., & Park, S. J. (2019). Recent advances in TiO_2 films prepared by sol-gel methods for photocatalytic degradation of organic pollutants and antibacterial activities. *Coatings*, *9*(10). https://doi.org/10.3390/coatings9100613

Yilleng, M.T., Avong, S.C., Stephen, D., Madaki, L.A., Akande, A.J. & Yakusak, N.S. (2019) Photocatalytic Degradation of Chlorazole Black E Dye using Silver Doped Titanium Dioxide. Nigerian Research Journal of Chemic al Sciences, *6*, 145–154.

Rafiq, A., Ikram, M., Ali, S., Niaz, F., Khan, M., Khan, Q., & Maqbool, M. (2021). Photocatalytic degradation of dyes using semiconductor photocatalysts to clean industrial water pollution. *Journal of Industrial and Engineering Chemistry*, *97*(February), 111– 128. https://doi.org/10.1016/j.jiec.2021.02.017

Razani, A., Abdullah, A. H., & Fitrianto, A. (2017). *Sol-Gel Synthesis of Fe_2 O_3 -Doped TiO 2 for Optimized Photocatalytic Degradation of 2 , 4-Dichlorophenoxyacetic Acid*. 1–10.

Saravanan, S., & Soga, T. (2021). *Study of pure and Ag-doped TiO_2 nanoparticles for photocatalytic degradation of methylene blue Study of pure and Ag-doped TiO $_2$ nanoparticles for photocatalytic degradation of methylene blue*. https://doi.org/10.1088/1757-899X/1033/1/012050

Shittu, H. A., Adedokun, O., Kareem, M. A., Bello, I. T., & Arumugam, S. (2023). *Effect of Low-Doping Concentration on Silver-Doped SnO_2 and its Photocatalytic Applications*. *13*(2), 1–15.

Shivaraju, H. P., Anil, G. M. K. M., & Pallavi, K. S. (2017). Degradation of selected industrial dyes using Mg-doped TiO_2 polyscales under natural sun light as an alternative driving energy. *Applied Water Science*. https://doi.org/10.1007/s13201-017-0546-0

Shukla, B. K., Rawat, S., Gautam, M. K., Bhandari, H., Garg, S., & Singh, J. (2022). Photocatalytic Degradation of Orange G Dye by Using Bismuth Molybdate: Photocatalysis Optimization and Modeling via Definitive Screening Designs. *Molecules*, *27*(7). https://doi.org/10.3390/molecules27072309

Solís-Casados, D. A., Escobar-Alarcón, L., Alvarado-Pérez, V., & Haro-Poniatowski, E. (2018). Photocatalytic activity under simulated sunlight of Bi-modified TiO2 thin films obtained by sol gel. *International Journal of Photoenergy*, *2018*. https://doi.org/10.1155/2018/8715987

Toxicol, J. E. A., Avasarala, B. K., Tirukkovalluri, S. R., & Bojja, S. (2016). *Environmental & Analytical Toxicology Magnesium Doped Titania for Photocatalytic Degradation of Dyes in Visible Light*. *6*(2). https://doi.org/10.4172/2161-0525.1000358

Xie, W., Li, R., & Xu, Q. (2018). Enhanced photocatalytic activity of Se-doped TiO_2 under visible light irradiation. *Scientific Reports*, 1–10. https://doi.org/10.1038/s41598-01827135-4